



## The Effect of B, Al, N, and P Impurities on the Electronic Structure of $\text{Si}_{0.3}\text{Sn}_{0.7}\text{Ge}$ alloy: A First-Principles Approach

Collins E. Ouserigha, (Ph.D.)  
Ayibapreye K. Benjamin, (Ph.D.)  
Niger Delta University, Nigeria

[Doi:10.19044/esj.2022.v18n3p186](https://doi.org/10.19044/esj.2022.v18n3p186)

Submitted: 04 October 2021  
Accepted: 26 December 2021  
Published: 31 January 2022

Copyright 2022 Author(s)  
Under Creative Commons BY-NC-ND  
4.0 OPEN ACCESS

*Cite As:*

Ouserigha E.C. & Benjamin A.K. (2022). *The effect of B, Al, N, and P impurities on the electronic structure of  $\text{Si}_{0.3}\text{Sn}_{0.7}\text{Ge}$  alloy: a first-principles approach*. European Scientific Journal, ESJ, 18 (3), 1.

<https://doi.org/10.19044/esj.2022.v18n3p186>

### Abstract

This study examines the effect of doping  $\text{Si}_{0.3}\text{Sn}_{0.7}\text{Ge}$  with an impurity element X (B, Al, N, or P) on the Sn site, using first-principle calculations based on the fully self-consistent Korringa-Kohn-Rostoker method with the coherent potential approximation (KKR-CPA). To treat several forms of chemical disorders of  $\text{Si}_{0.3}\text{Sn}_{0.7}\text{Ge}$ , X-doping was carried out by substituting small amounts of Sn with each element X, which gives rise to the alloy  $\text{Si}_{0.3}\text{Sn}_{0.7-y}\text{X}_y\text{Ge}$ . As the X content increases from  $y = 0.01$  to 0.06, the Fermi level maintains its position in the conduction band edge. While the number of states at the Fermi level decreases. With 1% X impurity added to the alloy  $\text{Si}_{0.3}\text{Sn}_{0.7-y}\text{X}_y\text{Ge}$ , the number of carriers (electron and hole) states was generally enhanced. For the case of  $X = \text{P}$ , when compared to the parent material  $\text{Si}_{0.3}\text{Sn}_{0.7}\text{Ge}$ , an enhancement of 0.04 states/eV was observed. Due to the increase in the number of states, which indicates an improvement in thermopower, these alloys  $\text{Si}_{0.3}\text{Sn}_{0.7-y}\text{X}_y\text{Ge}$  are promising for application as n-type electrodes in a thermoelectric generator (TEG).

**Keywords:** First-principles, chemical disorders, thermopower, thermoelectric generator, KKR-CPA.

## 1.0. Introduction

SiGe-based alloys are a promising material for thermoelectric devices such as a micro-energy generator for wearable and portable electronics (Peng *et al.*, 2019; Francioso *et al.*, 2011). SiGe compounds have the advantage of being widely available, inexpensive, and non-toxic. So, there is an increasing interest to use SiGe alloys in thermoelectric generators. A thermoelectric generator (TEG) converts heat into electricity through a temperature difference between two sides of the device. The efficiency of such a device depends on the thermoelectric material's figure of merit  $ZT$ , which is a dimensionless quantity. This in turn depends on the product of the square of the Seebeck coefficient and electrical conductivity ( $\alpha^2\sigma$ ), called the thermopower. Hence, to get an efficient TEG, the thermopower of the thermoelectric material should be high.

It is generally known that to increase the  $ZT$  values of a thermoelectric material, the Seebeck coefficient and electrical conductivity need to be high, while, the thermal conductivity has to be low. So, a high Seebeck coefficient and electrical conductivity indicates an enhancement in the thermopower. An improvement in thermopower can be achieved through an increase in the electronic density of state (DOS) at the Fermi level (Chen *et al.*, 2012; He & Tritt, 2017). One of the ways of increasing the thermopower is through bandstructure engineering (He & Tritt, 2017), which has to do with tuning the electronic structure of the promising material by adding impurity elements to it.

Motivated by the works of Peng *et al.*, 2019 and Bhogra *et al.*, 2019, that through ion implantation, the thermoelectric properties of materials can be tuned (Peng *et al.*, 2019; Bhogra *et al.*, 2019). And the promising results from the work of Ouserigha and Ogobiri (2021), where the addition of one percent Boron (B) impurity to the SiGe-based alloy,  $\text{Si}_{0.3}\text{Sn}_{0.7}\text{Ge}$  lead to an increase in the number of carrier states. Here, a small amount of impurity elements X (1 to 6%) from group III (Boron {B} and Aluminium {Al}) and group V (Nitrogen {N} and Phosphorus {P}) of the periodic table are added to the  $\text{Si}_{0.3}\text{Sn}_{0.7}\text{Ge}$  alloy on the Si site. The systems were modeled with the spin-polarized relativistic Korringa-Kohn-Rostoker (SPR-KKR) density functional theory code (Ebert *et al.*, 2011). The simulation results show that the alloys  $\text{Si}_{0.3}\text{Sn}_{0.69}\text{B}_{0.01}\text{Ge}$ ,  $\text{Si}_{0.3}\text{Sn}_{0.69}\text{Al}_{0.01}\text{Ge}$ ,  $\text{Si}_{0.3}\text{Sn}_{0.69}\text{N}_{0.01}\text{Ge}$ , and  $\text{Si}_{0.3}\text{Sn}_{0.64}\text{P}_{0.06}\text{Ge}$  has the highest number of carrier states.

## 2.0. Computational Method

The atomic positions in the conventional unit cell of zinc-blende SiGe (space group  $F\bar{4}3m$ ) are given by the Wyckoff position  $4a$  (0, 0, 0) for Si atom and  $4c$  (0.25, 0.25, 0.25) for Ge atom. This conventional unit cell of SiGe with lattice parameter  $a = 10.5825$  a.u is shown in figure 2.1. For the impurity-

doped systems,  $\text{Si}_{0.3}\text{Sn}_{0.7-y}\text{X}_y\text{Ge}$ , element X (B, Al, N, and P) was inserted into the Sn site to form the new alloys. Where  $y$  represents the doping concentration with values from 0.01 to 0.06.

The calculations were performed using the Korringa-Kohn-Rostoker Green's function (KKR-GF) method as implemented in the Munich spin-polarized relativistic Korringa-Kohn-Rostoker (SPR-KKR) code (Ebert *et al.*, 2011). KKR-GF method is an all-electron electronic structure method that provides direct access to the electronic Green's Function (GF) and uses a minimal, numerical and energy-dependent basis set. Is an accurate and flexible method to study a wide range of systems and properties in electronic structure theory. In the KKR-GF method, GF plays the central role and the single-particle GF is used as the starting point of the calculation. To perform the simulations, we used the local density approximation – Vosko, Wilk, Nusair (LDA-VWN) exchange-correlation functional (Vosko *et al.*, 1980) throughout the calculations. The coherent potential approximation (CPA) is implemented for the chemically disordered systems. In the self-consistent field (SCF) calculations, a full potential spin-polarized relativistic Korringa-Kohn-Rostoker (FP-SPR-KKR) calculation was set up with a  $25 \times 25 \times 25$   $k$ -mesh grid (which generates 2119  $k$ -points) and energy (E)-mesh points of 50 Ry. Broyden's second method has been implemented for the SCF algorithm. An angular momentum expansion ( $l_{\max}$ ) of two was used.

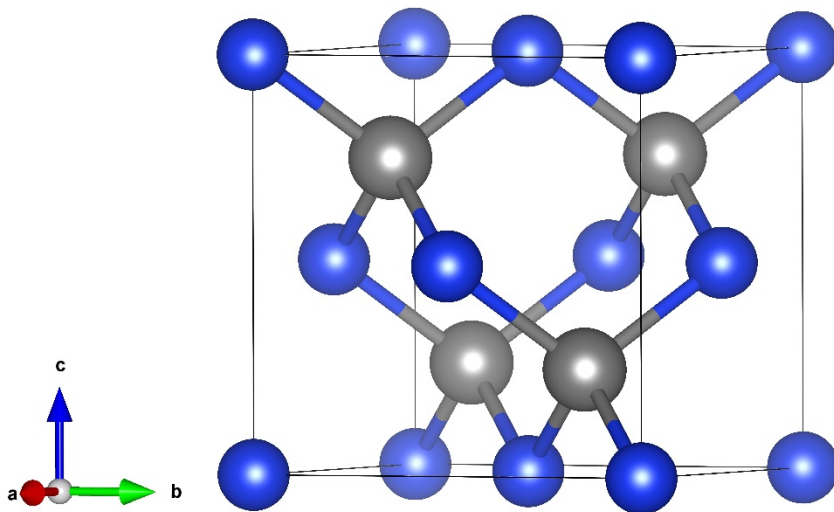


**Figure 2.1.** Cubic structure of SiGe. Blue (small) spheres represent Si atoms at position (0, 0, 0) while gray (large) spheres represent Ge atoms at position (0.25, 0.25, 0.25).

### 3.0. Discussion of Results

With the introduction of each impurity element X (B, Al, N, and P) into  $\text{Si}_{0.3}\text{Sn}_{0.7-y}\text{X}_y\text{Ge}$  with the impurity concentration  $y$  varying from 0.01 to

0.06, several robust n-type thermoelectric alloys were formed. These alloys are  $\text{Si}_{0.3}\text{Sn}_{0.7-y}\text{B}_y\text{Ge}$ ,  $\text{Si}_{0.3}\text{Sn}_{0.7-y}\text{Al}_y\text{Ge}$ ,  $\text{Si}_{0.3}\text{Sn}_{0.7-y}\text{N}_y\text{Ge}$ , and  $\text{Si}_{0.3}\text{Sn}_{0.7-y}\text{P}_y\text{Ge}$ , whose total density of state (dos) plots are given in figures 3.1 to 3.4. The small amount of group III or V impurities introduced into the Sn site can lead to improvement in the power factor. And when the number of states is high from the dos plots (figures 3.1 to 3.4) for a given impurity concentration, it indicates that the power factor is also high for that particular alloy. Increasing the amount of X impurity from 0.01 to 0.06 with a step increment of 0.01 did not affect the conductivity type. The n-type conductivity of the parent alloy  $\text{Si}_{0.3}\text{Sn}_{0.7}\text{Ge}$  was maintained by the newly formed alloys and an increase in the total number of electronic states was observed. With an increase in the number of states at the Fermi level, the thermopower of the materials will improve and they can be used as an n-type material in a thermoelectric device.

Figures 3.1, 3.2, 3.3, and 3.4 show the total DOS plots, respectively, for the  $\text{Si}_{0.3}\text{Sn}_{0.7-y}\text{B}_y\text{Ge}$ ,  $\text{Si}_{0.3}\text{Sn}_{0.7-y}\text{Al}_y\text{Ge}$ ,  $\text{Si}_{0.3}\text{Sn}_{0.7-y}\text{N}_y\text{Ge}$ , and  $\text{Si}_{0.3}\text{Sn}_{0.7-y}\text{P}_y\text{Ge}$  alloys. In each of these figures, the graphs (a) through (f) represent the DOS plots for the impurity concentration  $y$  as it increases from 0.01 through 0.06 in the interval 0.01. For the alloy systems  $\text{Si}_{0.3}\text{Sn}_{0.7-y}\text{B}_y\text{Ge}$ ,  $\text{Si}_{0.3}\text{Sn}_{0.7-y}\text{Al}_y\text{Ge}$ , and  $\text{Si}_{0.3}\text{Sn}_{0.7-y}\text{N}_y\text{Ge}$ , as the amount of impurity concentration  $y$  increases from 0.01 to 0.06, the number of carrier (electron and hole) states per unit volume per energy decreases as shown in table 1. While in the case of  $\text{Si}_{0.3}\text{Sn}_{0.7-y}\text{P}_y\text{Ge}$  an increase in the impurity concentration results in an increase in the total number of carrier states (see table 1).

From table 1, we can see that the highest value for the carrier states is 0.264 states/eV and the alloy that produces this value is  $\text{Si}_{0.3}\text{Sn}_{0.64}\text{P}_{0.06}\text{Ge}$ . Also, when 1% of the impurity atoms of B, Al, N was introduced into the Sn site of  $\text{Si}_{0.3}\text{Sn}_{0.7}\text{Ge}$ , the following alloys were formed:  $\text{Si}_{0.3}\text{Sn}_{0.69}\text{B}_{0.01}\text{Ge}$ ,  $\text{Si}_{0.3}\text{Sn}_{0.69}\text{Al}_{0.01}\text{Ge}$ , and  $\text{Si}_{0.3}\text{Sn}_{0.69}\text{N}_{0.01}\text{Ge}$ . These alloys have an increased number of carrier states as can be seen in Table 1 when compared to the computed carrier states of 0.117 states/eV for the parent alloy  $\text{Si}_{0.3}\text{Sn}_{0.7}\text{Ge}$  (Ouserigha and Ogobiri, 2021). With an improvement in their carrier states, it means the conductivities of these alloys will increase, making them promising n-type materials for a TEG.

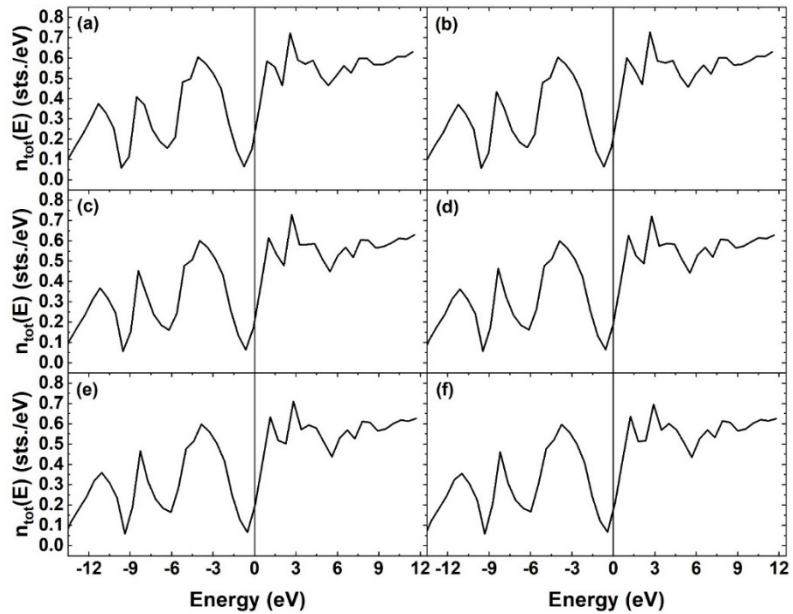


**Figure 3.1.** Total DOS of  $\text{Si}_{0.3}\text{Sn}_{0.7}\text{Ge}$  doped with Boron impurities for a varying amount of concentration  $y$ . Impurity concentration  $y$  is from 0.01 to 0.06, which is respectively given in figures (a) to (f).

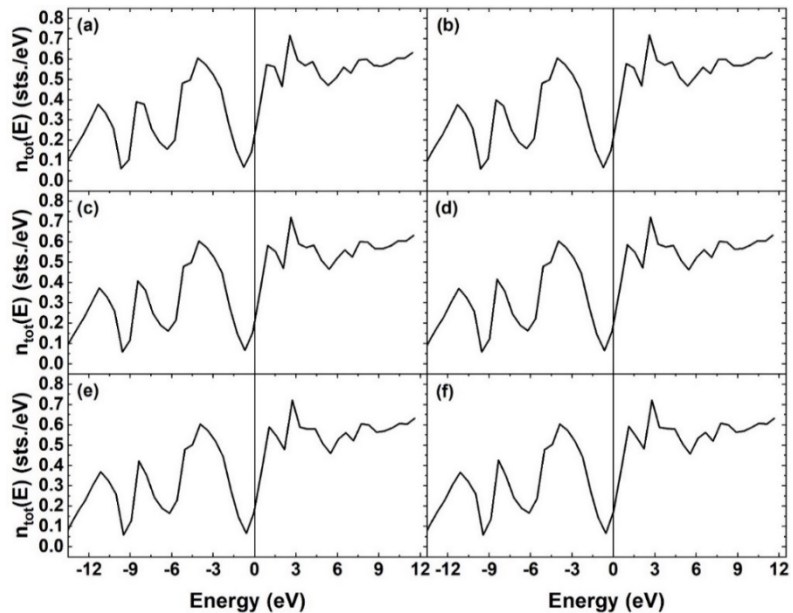


**Figure 3.2.** Total DOS of  $\text{Si}_{0.3}\text{Sn}_{0.7}\text{Ge}$  doped with Aluminium impurities for a varying amount of concentration  $y$ . Impurity concentration  $y$  is from 0.01 to 0.06, which is respectively given in figures (a) to (f).

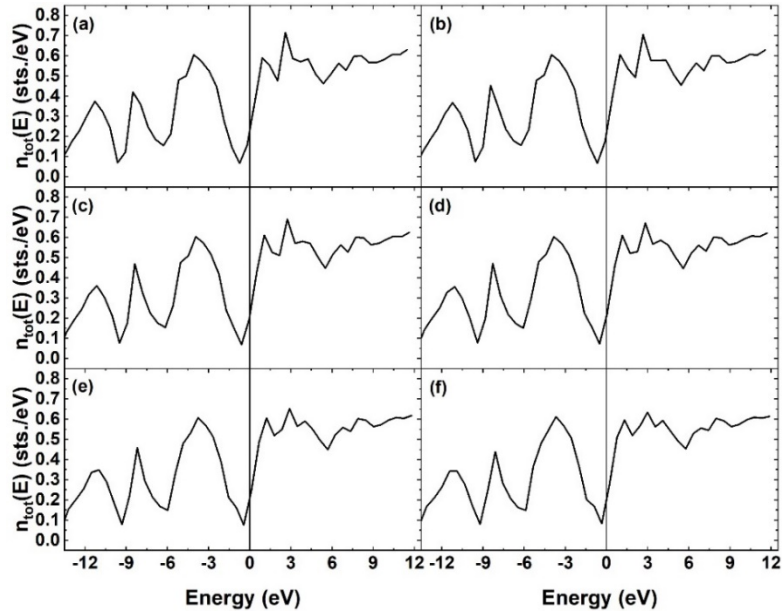


**Figure 3.3.** Total DOS of  $\text{Si}_{0.3}\text{Sn}_{0.7}\text{Ge}$  doped with Nitrogen impurities for a varying amount of concentration  $y$ . Impurity concentration  $y$  is from 0.01 to 0.06, which is respectively given in figures (a) to (f).

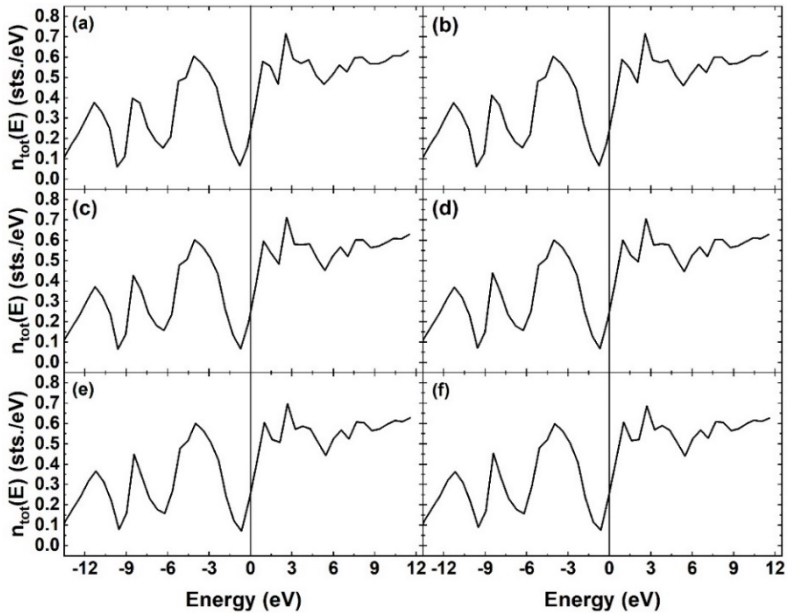


**Figure 3.4.** Total DOS of  $\text{Si}_{0.3}\text{Sn}_{0.7}\text{Ge}$  doped with Phosphorus impurities for a varying amount of concentration  $y$ . Impurity concentration  $y$  is from 0.01 to 0.06, which is respectively given in figures (a) to (f).

**Table 1.** Total number (No.) of the carrier (electron and hole) states at the Fermi level ( $E_F$ ) for the alloy systems  $Si_{0.3}Sn_{0.7-y}B_yGe$ ,  $Si_{0.3}Sn_{0.7-y}Al_yGe$ ,  $Si_{0.3}Sn_{0.7-y}N_yGe$ , and  $Si_{0.3}Sn_{0.7-y}P_yGe$ .

S/N	Amount of impurity Conc. y	Total No. of States at $E_F$ for $Si_{0.3}Sn_{0.7-y}B_yGe$	Total No. of States at $E_F$ for $Si_{0.3}Sn_{0.7-y}Al_yGe$	Total No. of States at $E_F$ for $Si_{0.3}Sn_{0.7-y}N_yGe$	Total No. of States at $E_F$ for $Si_{0.3}Sn_{0.7-y}P_yGe$
1	0.01	0.227	0.228	0.231	0.241
2	0.02	0.217	0.218	0.223	0.246
3	0.03	0.207	0.208	0.217	0.251
4	0.04	0.198	0.197	0.210	0.255
5	0.05	0.193	0.184	0.210	0.259
6	0.06	0.183	0.171	0.203	0.264

## Conclusion

Density functional theory studies have been carried out on  $Si_{0.3}Sn_{0.7-y}X_yGe$  ( $X = B, Al, N, P$ ) using the full potential relativistic Korringa-Kohn-Rostoker Green function (KKR-GF) method as implemented in the Munich SPR-KKR simulation software. Analysis of the density of states plots of these alloys indicates that they all maintain the n-type conductivity of the parent alloy  $Si_{0.3}Sn_{0.7}Ge$  and some of them show an increased number of carrier states when a small quantity of the dopant X is added. These features can be seen in figures 3.1 to 3.4, where the dip of the curve around the Fermi level (the zero mark on the energy axis) is located on the left side of the fermi level and the point where the curve cuts through the Fermi level indicates the carrier states per electron-volt (eV). With 1% of the impurity element X (for  $X = B, Al,$  and  $N$ ) added to form the alloys;  $Si_{0.3}Sn_{0.69}B_{0.01}Ge$ ,  $Si_{0.3}Sn_{0.69}Al_{0.01}Ge$ , and  $Si_{0.3}Sn_{0.69}N_{0.01}Ge$ , the highest number of carrier states, respectively given as 0.227, 0.228, and 0.231 states/eV was reached. While the highest number of carrier states of 0.264 states/eV for the alloy  $Si_{0.3}Sn_{0.64}P_{0.06}Ge$  was achieved at 6% P impurity added to  $Si_{0.3}Sn_{0.7-y}X_yGe$  (see table 1). The high carrier states observed for these materials are an indication that their electrical conductivity and Seebeck coefficient have increased. Which makes these alloys ( $Si_{0.3}Sn_{0.69}B_{0.01}Ge$ ,  $Si_{0.3}Sn_{0.69}Al_{0.01}Ge$ ,  $Si_{0.3}Sn_{0.69}N_{0.01}Ge$ , and  $Si_{0.3}Sn_{0.64}P_{0.06}Ge$ ) possible candidates for application as an n-type thermoelectric material. SiGe-based n-type electrode for TEGs has not been studied widely and quaternary compounds made by ion implantation have been shown to increase the thermoelectric performance of a thermoelectric material (Bhogra *et al.*, 2019; Peng *et al.*, 2019). This research work has

contributed to existing knowledge by supporting the work of Peng *et al.*, 2019 and has shown other possible alloys ( $\text{Si}_{0.3}\text{Sn}_{0.69}\text{Al}_{0.01}\text{Ge}$ ,  $\text{Si}_{0.3}\text{Sn}_{0.69}\text{N}_{0.01}\text{Ge}$ , and  $\text{Si}_{0.3}\text{Sn}_{0.64}\text{P}_{0.06}\text{Ge}$ ) that can be made via implanting Al, N, P ion in a SiGe based thermoelectric material.

### Acknowledgment

The authors are grateful to Dr. Nimibofa Ayawei for his useful deliberations and the financial support received towards this research work. In addition, the authors appreciate the insightful comments from the reviewers and the editor-in-chief.

### References:

1. Bhogra, A., Masarrat, A., Meena, R., Hasina, D., Bala, M., Dong, C. L., Chen C., Som T., Kumar A., & Kandasami, A. (2019). Tuning the electrical and thermoelectric properties of N ion implanted  $\text{SrTiO}_3$  thin films and their conduction mechanisms. *Scientific Reports*, 9(1), 1-11.
2. Chen, Z. G., Han, G., Yang, L., Cheng, L., & Zou, J. (2012). Nanostructured thermoelectric materials: Current research and future challenge. *Progress in Natural Science: Materials International*, 22(6), 535-549.
3. Ebert, H., Koedderitzsch, D., & Minar, J. (2011). Calculating condensed matter properties using the KKR-Green's function method—recent developments and applications. *Reports on Progress in Physics*, 74(9), 096501.
4. Francioso, L., De Pascali, C., Farella, I., Martucci, C., Cretì, P., Siciliano, P., & Perrone, A. (2011). Flexible thermoelectric generator for ambient assisted living wearable biometric sensors. *Journal of Power Sources*, 196(6), 3239-3243.
5. He, J., & Tritt, T. M. (2017). Advances in thermoelectric materials research: Looking back and moving forward. *Science*, 357(6358).
6. Ouserigha, C. E., & Ogobiri, G. E. (2021, April). First-principles investigation of the electronic and thermoelectric properties of SiGe doped with Sn and one percent B. In *IOP Conference Series: Earth and Environmental Science* (Vol. 730, No. 1, p. 012001). IOP Publishing.
7. Peng, Y., Miao, L., Gao, J., Liu, C., Kurosawa, M., Nakatsuka, O., & Zaima, S. (2019). Realizing High Thermoelectric Performance at Ambient Temperature by Ternary Alloying in Polycrystalline  $\text{Si}_{1-x}\text{Ge}_x\text{Sn}_y$  Thin Films with Boron Ion Implantation. *Scientific Reports*, 9(1), 1-9.

8. Vosko, S. H., Wilk, L., & Nusair, M. (1980). Accurate spin-dependent electron liquid correlation energies for local spin density calculations: a critical analysis. *Canadian Journal of Physics*, 58(8), 1200-1211.